PROCEEDINGS B

Research

CrossMark
click for updates

Author for correspondence:
M. Concetta Morrone
e-mail: concetta@in.cnr.it

THE ROYAL SOCIETY
PUBLISHING

Rhythmic modulation of visual contrast discrimination triggered by action

Alessandro Benedetto[1,2,3], Donatella Spinelli[4,5] and M. Concetta Morrone[2,6]

[1]Department of Neuroscience, Psychology, Pharmacology and Child Health, University of Florence, 50135 Florence, Italy
[2]Department of Translational Research on New Technologies in Medicines and Surgery, University of Pisa, Via San Zeno 31, 56123 Pisa, Italy
[3]Institute of Neuroscience, National Research Council (CNR), 56124 Pisa, Italy
[4]Department of Human Movement, Social and Health Sciences, University of Rome, 'Foro Italico', Pizza Lauro De Bosis 15, 00135, Rome, Italy
[5]IRCCS Santa Lucia Foundation, Rome, Italy
[6]Scientific Institute Stella Maris, Viale del Tirreno 331, 56018 Calambrone, Pisa, Italy

AB, 0000-0002-9713-1300; DS, 0000-0002-4890-6931; MCM, 0000-0002-1025-0316

Recent evidence suggests that ongoing brain oscillations may be instrumental in binding and integrating multisensory signals. In this experiment, we investigated the temporal dynamics of visual–motor integration processes. We show that action modulates sensitivity to visual contrast discrimination in a rhythmic fashion at frequencies of about 5 Hz (in the theta range), for up to 1 s after execution of action. To understand the origin of the oscillations, we measured oscillations in contrast sensitivity at different levels of luminance, which is known to affect the endogenous brain rhythms, boosting the power of alpha-frequencies. We found that the frequency of oscillation in sensitivity increased at low luminance, probably reflecting the shift in mean endogenous brain rhythm towards higher frequencies. Importantly, both at high and at low luminance, contrast discrimination showed a rhythmic motor-induced suppression effect, with the suppression occurring earlier at low luminance. We suggest that oscillations play a key role in sensory–motor integration, and that the motor-induced suppression may reflect the first manifestation of a rhythmic oscillation.

1. Introduction

Ongoing brain oscillations modulate perception, suggesting that sensory systems act as discrete mechanisms sampling information from the environment within specific time-windows [1–3]. Several electrophysiological studies have demonstrated that neural oscillations preceding the sensory stimulation are causally linked to perceptual performance [4–7]. Oscillations have also been demonstrated in perceptual performance after the presentation of a sensory stimulation [8–10]. These results can be interpreted as a synchronization of the endogenous rhythms of the visual brain by the preceding stimulus, or as a gain modulation owing to the stimulus-driven attention that oscillates over time [11]. Whatever the underlying mechanism, oscillatory fluctuation of sensory sensitivity could play a major role in aligning a temporal incoherent flow of sensory events, contributing to the integration of information from different sensory modalities. Similar integration mechanisms may also mediate the synchronization between action and perception, where temporal alignment is critical. Although the visual system has developed a selective pathway to dialogue optimally with action [12], a visual–motor synchronization mechanism is still needed, and sensory oscillations may facilitate this difficult task [13–15]. Recently, Wood *et al.* [16] have shown that a visual stimulus can reset the phase of alpha oscillations in the skeletomotor periphery. Complementary, Tomassini *et al.* [2] showed that action preparation synchronizes visual oscillations in the theta-band, possibly via a coupling between early motor planning and early visual processing. Interestingly, the coupling is independent of the spatial congruency between the visual stimulus and the action, as well as on the kinematics of the movement.

The aim of this study was to investigate the fine temporal dynamics of visual–motor integration processes. First, we asked whether a simple voluntary motor 'go' signal could synchronize visual oscillations and, if so, how long they would persist; second, whether the frequency of visual oscillations could be changed by manipulating the endogenous brain rhythms or the neural temporal characteristics of visual processing. To address the second question, we reduced the ambient luminance from photopic to mesopic level. The latency and integration time of visual processing increases at low luminance, and the effect is already present at retinal level, becoming stronger at later processing sites. If oscillations are linked to the dynamics of the neuronal response, then we predict a decrease in the oscillation frequency: the temporally prolonged responses to visual inputs in the dark should reduce the capability to modulate cortical discharge at high frequencies. On the other hand, we should expect a shift of the perceptual rhythm towards higher frequency, if the oscillations reflect the brain endogenous rhythm that is known to increase in frequency, at low luminance [17,18]. Our data, being consistent with the second hypothesis, suggest that visual oscillations are a consequence of the network dynamic properties. They further suggest that the phase-locking mechanisms do not depend on visual stimulus processing time.

2. Material and methods

(a) Participants

Eight volunteers (three women; mean age: 27 ± 3 years; including one author) performed the experiments. All had normal or corrected-to-normal vision. Participants provided an informed consent in accordance with the Declaration of Helsinki (2008).

(b) Apparatus

For experiment 1, stimuli and responses were generated and recorded using the ViSaGe and CB6 response box (Cambridge Research Systems) controlled via CRS Toolbox for MATLAB and presented on a Barco Calibrator monitor with a resolution of 800×600 pixels and a refresh rate of 120 Hz, mean luminance of 38.5 cd m^{-2}, ambient light approximately 0.08 cd m^{-2}. For experiment 2, stimuli and responses were generated and recorded by the MATLAB psychtoolbox [19] and presented on a CRT monitor with a resolution of 800×600 pixels and a refresh rate of 85 Hz, mean luminance of 51.8 cd m^{-2}, ambient light approximately 0.01 cd m^{-2}. In the low-luminance experimental condition, neutral filters of 1.5 LU were mounted on the goggles worn by the participants. Monitors ($40 \times 30°$, viewing distance 57 cm) were gamma calibrated, and the physical fluctuations of contrast throughout the trial duration were too small to be measured by a photometer.

(c) Stimuli and procedure

Participants maintained fixation on a central red square ($0.25°$) appearing at the beginning of the block and lasting until the end of the session. The stimulus was a horizontal sinusoidal grating (1c per degree, contrast 10%) presented with random phase for one frame through a $5°$ circular window of smoothed edge. In the upper or lower half of the circular window, a contrast increment was obtained by boosting the sinusoidal amplitude in an ellipsoidal Gaussian window (see equation in the electronic supplementary material).

In the *self-trigger* conditions, participants pressed a button to initiate the trial. After a random delay between 0 and 1 s, the stimulus was displayed, and the subjects reported the location of the contrast increment. To avoid the response action perturbing visual oscillations, subjects were required to delay the response for 2 s after the stimulus presentation in experiment 1 and 0.3 s in experiment 2. In experiment 1, participants had to pause for at least 2 s before pressing again the button to start the next trial; in experiment 2, they had to wait 0.3 s. In the *self-trigger* conditions, data were acquired at high luminance (*self-HL*) and with neutral filters (*self-LL*).

To evaluate the contribution of biological noise and possible stimulus contrast fluctuation to the oscillation in performance, we repeated experiment 1 with a random trigger (hereafter *random-HL*): the stimulus onset was randomly delivered by the computer between 3 and 7 s after the response, mimicking the temporal event sequence of the *self-trigger* conditions. This task was performed only at high luminance. Also in this condition, participants were asked to wait 2 s after stimulus presentation before responding. In experiment 2, we replicated both *self-trigger* conditions of experiment 1, adding a third condition, where the trigger was a sound. The auditory condition was performed under high-luminance viewing (hereafter called *audio-HL*), and participants were instructed to attend to the auditory cue (noise burst, 12 ms duration). The visual stimulus was presented after a random delay (0–1 s) from the auditory cue. The auditory cue was delivered via external speakers. The intertrial interval randomly varied between 0.3 and 0.8 s, mimicking the intertrial interval of the *self-trigger* conditions for experiment 2. To optimize sampling, in experiment 2, the majority (80% of total trials) of stimulus delays were in the first 350 ms from the trigger onset. An auditory feedback informed participants that they did not respect the required delay before responding. These trials were removed from further analysis. No other feedback was provided. Subjects were required to keep tactile contact with the response box throughout the experiment.

A QUEST procedure was adopted to obtain individual psychometric functions of contrast increment sensitivity. The contrast increment value that elicited about 75% of correct responses was selected and kept constant within each block. In order to balance perceptual learning improvement, the contrast increment was slightly adjusted from block to block to maintain the 75% of correct responses. In experiment 1, the average number of trials per subject collected over 3–7 sessions were 794 ± 377; in experiment 2, these were reduced at 511 ± 121, given that we collected trials limited to delays ranging from 12 to 350 ms. The number of independent trials for each delay are shown in the figures. If not stated differently, then the number of trials contributing to the bin average was double of those plotted, given the 50% overlap between bins.

(d) Data analysis

To evaluate the presence of an oscillation, we performed several analyses both at individual level and by pooling individual data together (hereafter termed *aggregate observer*, as in [20]) or by group-average in experiment 2.

For experiment 1, we calculated the percentage of correct responses in 50 ms bins that overlapped by 50% with the adjoining one. The variability was assessed via a bootstrap procedure (1000 iterations, with replacement and standard deviation of the bootstrap reported as standard error of the mean, s.e.m.). The time series were fitted with a sinusoidal function for each condition for the aggregate observer (equation reported in the electronic supplementary material). The best-fit statistical significance was evaluated using a bootstrap procedure on surrogated data: the delay of each trial of each subject was scrambled randomly, averaged and fitted with the same sinusoidal function used for the aggregate subject [8]. A one-tail non-parametric bootstrap t-test was run to assess if the adjusted-R^2 of the best fit of the data was statistically higher than the 95% of the adjusted-R^2 distribution obtained from the bootstrapped surrogate data.

To evaluate the power spectra of the aggregate observer, we performed a Fourier analysis in the range 3–8.5 Hz, with increments of 0.25 Hz. We averaged the temporal series of performance at the fixed interval under exam; we first binned the trials into seven contiguous intervals per period to optimize the number of trials
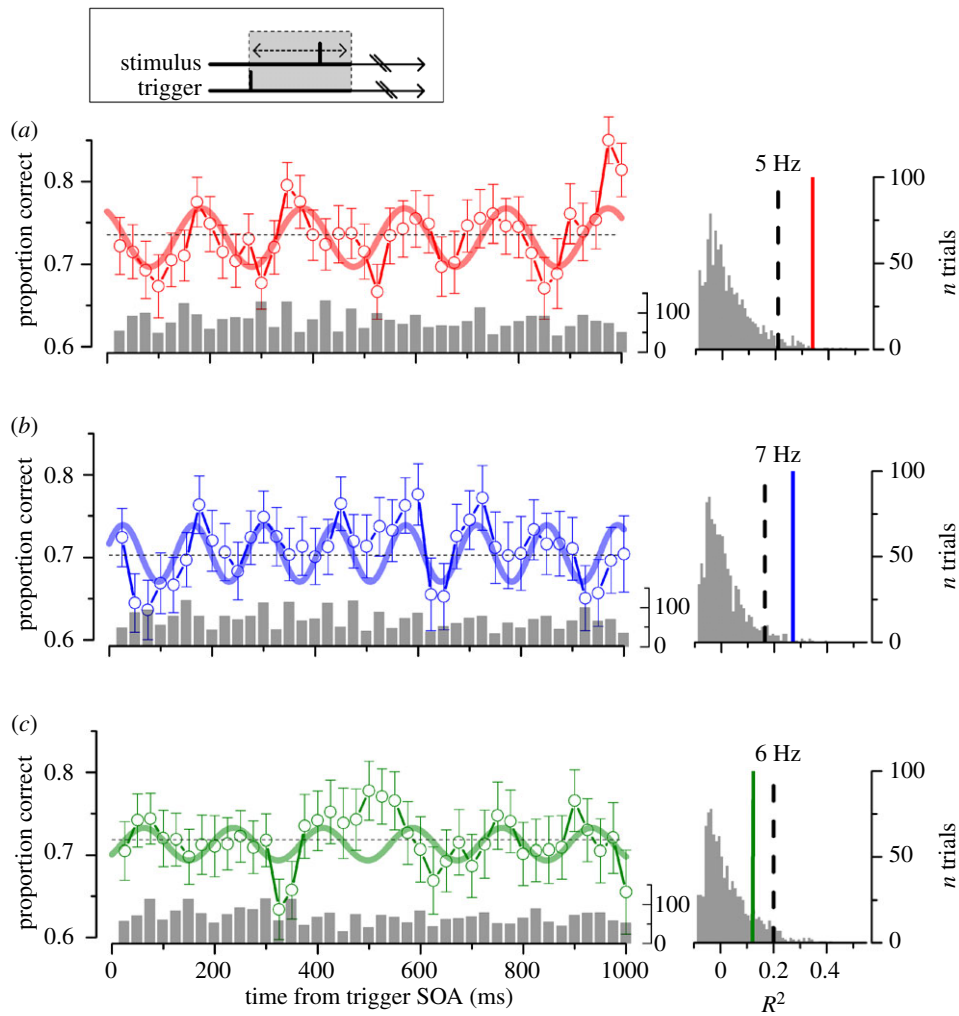
Figure 1. Left: contrast discrimination performance as function of delay (stimulus onset asynchrony, SOA) from the *self-trigger* condition at high-luminance (*a*, *self-HL*; red) and at low-luminance (*b*, *self-LL*, blue); *random-trigger* condition at high-luminance (*c*, *random-HL*, green). Aggregate observer, $n = 5$. Bar plots show the number of independent observations for each bin (on average 74 ± 23). Vertical lines represent the s.e.m. from bootstrapping; thick lines represent the best sinusoidal fit to the data; horizontal dashed lines represent the average correct response. Right: adjusted-R^2 distribution obtained by fitting the random shuffled data with the sinusoidal functions of *a*, *b* and *c*, respectively. Dashed lines mark 0.95 probability; thick lines mark the R^2 for *self-HL* ($p = 0.005$), *self-LL* ($p = 0.008$) and *random-HL* condition ($p = 0.12$). (Online version in colour.)

per bin and then evaluated the sinusoidal harmonic that best fitted the binned data. A two-dimensional statistical significance test was run on the real and imaginary components of fundamental harmonic in the frequency range between 3 and 8.5 Hz by bootstrap. A non-parametric one-tail sign test was run to determine whether the distribution of data points was different from zero in at least one of the components ($\alpha = 0.05$), implying that the two-dimensional cloud of bootstrapped data was not centred at the origin. To evaluate the presence of oscillations at individual level, we repeated the same analysis using six bins per period to optimize the number of trials per bin and we restricted the frequency to the range where the aggregate observer data were statistically significant.

3. Results

We measured how contrast discrimination accuracy varied as a function of delay of the motor-go signal in the *self-HL* condition (figure 1*a*), pooling together the data of all subjects in the aggregate observer. Performance is not constant over time but it oscillates for up to 1 s after the movement onset. The difference between the peaks and the troughs performance is more than 2 standard deviations. To assess whether oscillations are not a consequence of biological noise fluctuations, we fitted the sensitivity data with sinusoidal waveform and

compared the goodness of fit with the same fit applied to surrogate data obtained by randomly shuffling the time presentation of each trial [8] (figure 1, right panel). The best fit for the *self-HL* condition was obtained at 5 Hz. This fit exceeds the 95% of the adjusted-R^2 distribution obtained by best fitting the random shuffled data with the same sinusoidal function, indicating a significant oscillation at this frequency (adj.-$R^2 = 0.35$; $p < 0.01$; figure 1*a*). Other frequencies close to 5 Hz provide a statistically significant fit, but not frequencies higher than 6 Hz (figure 2).

To verify whether voluntary action was crucial in synchronizing oscillations, discrimination performance was measured when participants did not perform the start action, but passively observed a stimulus that was presented randomly (*random-HL*) with a delay of at least 3 s after the preceding response. Figure 1*c* shows the aggregate observer accuracy data for this condition. The best-fit was obtained at 5.9 Hz; however, the adjusted-R^2 was low and confined below the 95% limit, indicating that the oscillation is not significantly different from random noise (adj.-$R^2 = 0.13$; $p > 0.05$). The overall variance of the temporal series for the *random-HL* is lower than that for the *self-HL* (9.5 versus 14.8, respectively). The reduced variance for the *random-HL* is consistent with the result of the statistical analysis reported in figure 1.
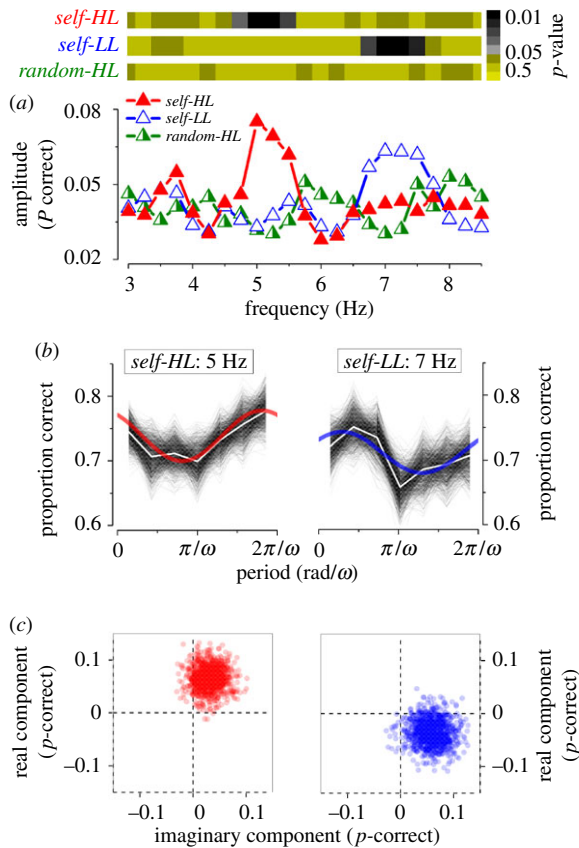
Figure 2. Spectral analysis of visual performance of the aggregate observer. (a) Bottom: amplitude for self-HL (red filled triangles), self-LL (blue empty triangles) and random-HL (green half-filled triangles) conditions. Top: statistical significance in colour code for the three conditions calculated by a two-dimensional cluster spread derived by bootstrap as shown in (c). (b) Spectral analysis applied to the most significant harmonic component for self-HL and self-LL (5 and 7 Hz respectively). Bootstrap simulations (thin lines), their mean (white line) and best-fit model (continuous thick line) for the self-HL and self-LL conditions. (c) Two-dimensional polar statistics for the two most significant frequencies analysed. Real and imaginary components of each bootstrap for the self-trigger conditions. Points clustered away from the origin, indicating statistical significance as reported in (a) top row. (Online version in colour.)

To investigate whether the frequency could be changed by manipulating the dynamics of the processing of temporal stimuli, we repeated the experiment at low-mesopic luminance (self-LL). Reliable oscillations were also detected at this luminance (figure 1b). However, the best-fitting sinusoidal function had a higher frequency than at photopic luminance, being now 7.1 Hz instead of 5 Hz observed at self-HL. Also for the self-LL condition, the one-tail bootstrap t-test revealed that the adjusted-R^2 distribution of the fit was significantly higher than noise level (adj.-$R^2 = 0.27$; $p < 0.01$). The fit of the low-luminance performance with a 5 Hz sinusoidal function was very poor (see also figure 2). Despite the fact that low luminance increases the processing latency of the sensory input, we observed an increase in frequency of the performance oscillation (see Discussion).

Figure 2a illustrates the Fourier transform of the time series in the range between 3 and 8.5 Hz. We calculated the amplitude at each frequency by averaging corresponding bins (fixed to 7 per period) for the various periods in the time series and best fitting the sinusoidal function. Examples of the procedure are shown in figure 2b for the most

representative frequencies of the aggregate observer for the self-trigger conditions. Black thin lines in figure 2b represent the probability of correct responses from each bootstrap iteration; white lines represent the mean; the best sinusoidal fit is superimposed in red for the self-HL and in blue for the self-LL condition, respectively. The average amplitude as function of frequency is reported in figure 2a (bottom panel). Self-HL (filled triangles) and self-LL (empty triangles) conditions show an amplitude peak around 5 and 7 Hz, respectively. The random-HL condition (half-filled triangles) shows lower amplitude across all frequencies. In order to estimate the significance of the oscillations, we run two-dimensional statistics, illustrated in figure 2c for the two most significant frequencies for the self-HL (5 Hz, left panels) and self-LL (7 Hz, right panels). Each point in figure 2c corresponds to the real and imaginary component of the best sinusoidal fit for each bootstrap iteration for the self-HL (red dots) and self-LL (blue dots) condition, respectively. The points cluster together away from the origin of the plot. Consistent with the previous analysis of figure 1, only a small range of frequencies around 5 Hz for the self-HL and around 7 Hz for the self-LL condition were higher than noise level (non-parametric one-tail sign test on the real or the imaginary component: self-HL: 5 Hz, $p = 0.003$; self-LL: 7 Hz, $p = 0.01$, figure 2a, top panel). No other frequencies reached significance level. Further, the amplitude of oscillations in the random-HL conditions was lower than noise at all frequencies.

The oscillations in the self-trigger conditions were strong enough to be detected also in individual subject data. Figure 3 shows the most significant frequencies for the individual subjects for the high- and low-luminance conditions in the range corresponding to those demonstrated for the aggregate observer (i.e. 4.8–5.5 Hz and 6.8–7.5 Hz, for self-HL and self-LL, respectively). Contrast discrimination accuracy oscillates significantly in this range for the majority of subjects for both conditions, with two exceptions which reached significance for only one of the two conditions. Subject S1 did not reach statistical significance for the self-HL condition and subject S5 did not reach statistical significance for the self-LL condition. The luminance-dependent shift of the oscillatory frequency was detected in almost all subjects, with higher frequency for the mesopic luminance.

Sensory signals are transiently suppressed in the first 100 ms after an action (motor-induced suppression; [21–23]). We investigated further the first 120 ms after action, to evaluate whether a similar transient effect can be detected in our paradigm. Figure 4a plots the same data of figure 1, now binned at 12 ms (50% overlap). Clearly, discrimination performance in both self-trigger conditions decreases around 100 ms after action (figure 4a). A two-tail binomial test revealed that the minimum performance points in the 0–120 ms range were lower than the average performance (self-HL: $p = 0.03$; self-LL: $p < 0.01$).

This suppression was confirmed at the individual level in experiment 2 where sampling was concentrated in the first 350 ms (see Methods and the electronic supplementary material, figure S3). Figure 4b shows group means for both self-HL (filled stars) and self-LL (empty stars) conditions. Replicating the finding from experiment 1, a two-tail binomial test confirmed that both self-HL and self-LL conditions showed a significant suppression in performance (self-HL: $p = 0.01$, self-LL: $p = 0.04$) in the first 120 ms from action execution. The latency of the individual minimum
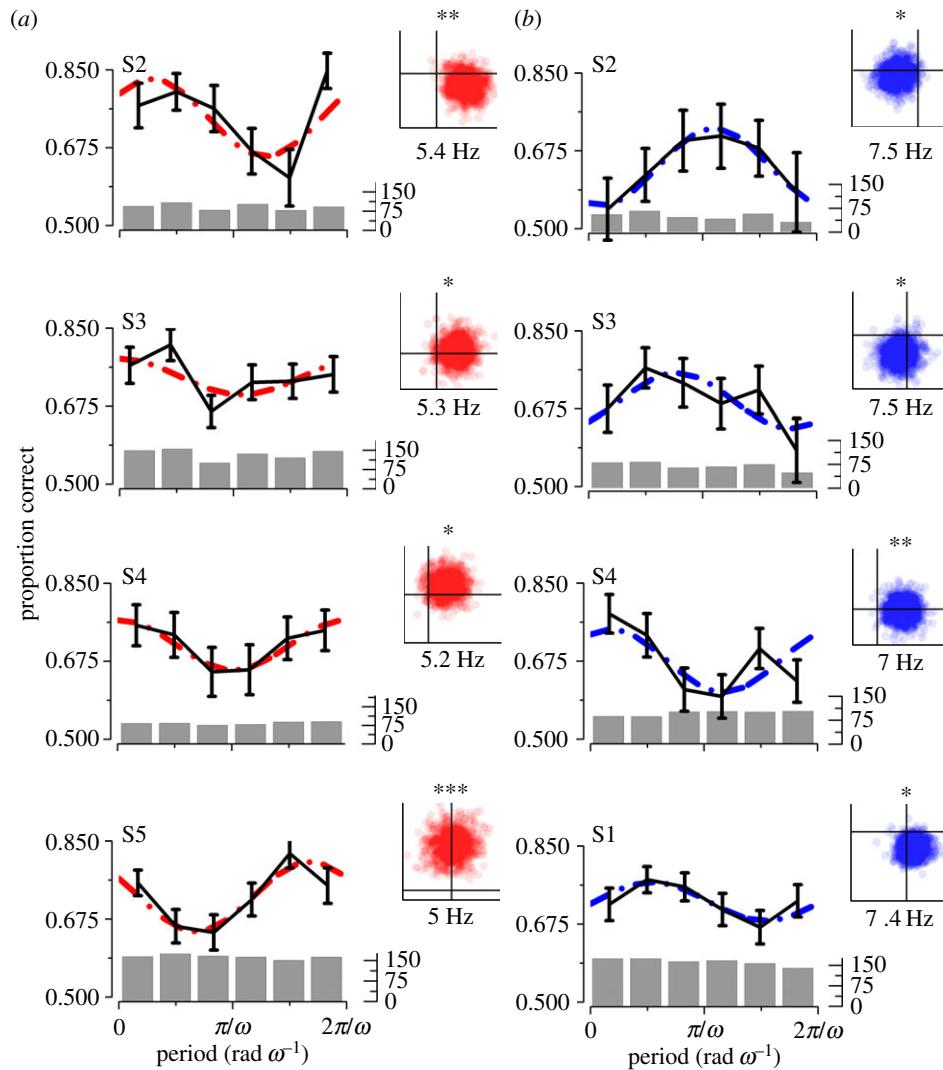
5

rspb.royalsocietypublishing.org Proc. R. Soc. B 283: 20160692

Figure 3. Single subject spectral analysis of visual performance in experiment 1 for *self-HL* (*a*) and *self-LL* (*b*) conditions. Each panel shows the most significant frequency modulation in the range between 4.8–5.5 and 6.8–7.5 for *self-HL* and *self-LL* respectively. Six equal bins for each frequency. Dashed lines: best-fit model. Black lines: means and s.e.m. Bar plot shows the number of independent observations for each bin. Insets on the left: the two-dimensional statistics for the individual frequencies, each point corresponds to a bootstrap iteration. *p*-values significant levels: 0.05*, 0.01** and 0.001***. (Online version in colour.)
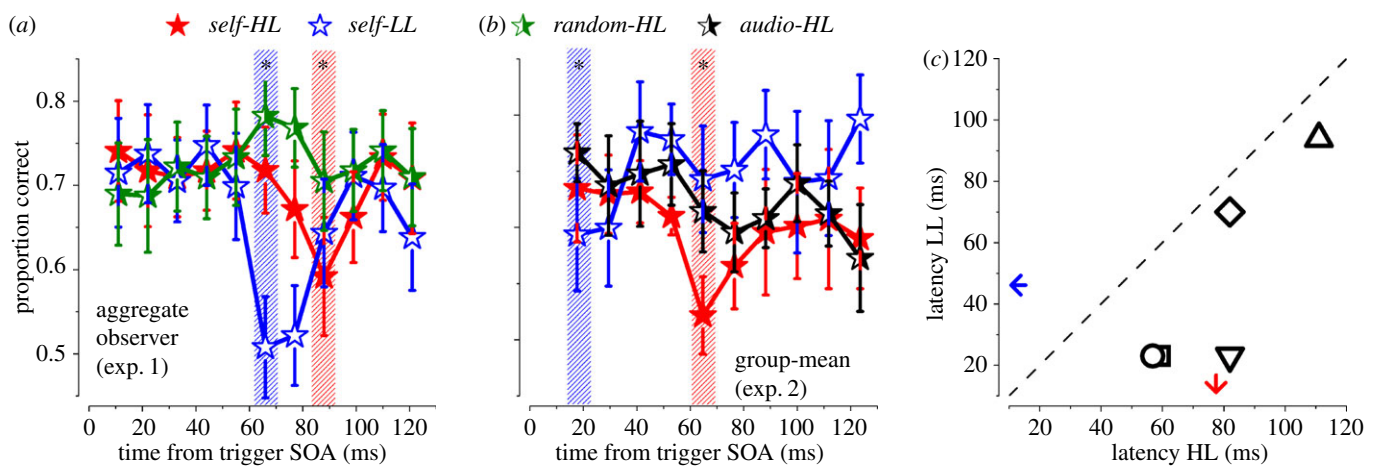

Figure 4. Proportion correct in the first 120 ms from trigger in experiments 1 and 2. (*a*) Aggregated observer results for experiment 1 ($n = 5$). (*b*) Group subject mean and s.e.m for experiment 2 ($n = 5$). Red filled stars: *self-HL*; Blue empty stars: *self-LL*; Green half-filled stars: *random-HL*; Black half-filled stars: *audio-HL*. Dashed bars indicate points statistically different from the mean of the curves (binomial test). Asterisk: $p < 0.05$. (*c*) Scatter plot of individual subjects' latency corresponding to the minimum performance for *self-HL* and *self-LL* conditions in experiment 2. The arrows indicate the means across subjects. All points are below the equality line, indicating the minimum performance is reached earlier at low than high luminance. Bin size is equal to 12 ms with 50% overlap. (Online version in colour.)

performance from experiment 2 scatter below the equality line (figure 4c), indicating that the minimum at the low-luminance was anticipated by about 30 ms with respect to the minimum at high-luminance (paired t-test(4) $= -4.22$, $p = 0.01$). Comparing the two experiments, there is an anticipation of the timing of both conditions in experiment 2, but the relative delay between the two conditions is similar.

The green curve (half-filled stars) of figure 4a replots at finer scale the data for the *random-HL* task of figure 1c. No data point was different from the mean in the first 120 ms, suggesting that the minimum performance observed in the two *self-trigger* conditions is not artefactual. To explore further the contribution of the motor component in producing the sensory suppression, we replaced the internal motor trigger with an external auditory trigger, keeping all other timing parameters constant. The black curve of figure 4b (half-filled stars, and the electronic supplementary material, figure S3) illustrates the group-mean for the *audio-HL* condition where we did not observe a statistically significant deviation from its mean in the first 120 ms ($p > 0.05$).

4. Discussion

We evaluated the effect of action and luminance on visual accuracy in a contrast-discrimination task. We confirm that action synchronizes theta-band oscillations of visual sensitivity [2]; in addition, we found three novel results. *First*, the action-synchronized oscillatory activity persists for up to 1 s after execution. *Second*, the oscillatory frequency varies with luminance within the theta range, i.e. the frequency is higher in mesopic than photopic vision. *Third*, action produces a sensory–motor suppressive effect in the first 100 ms earlier in time at low-luminance compared with high-luminance.

We found that button-press synchronizes visual oscillations in the theta range for up to 1 s from action onset. Oscillations emerged also at the group-level analysis, suggesting commonalities in oscillatory frequency and phase across participants. Crucially, no significant oscillations were detected when the stimulus was randomly delivered in the absence of a motor act, suggesting a link between the phase-locking signal and the motor act. Congruently, theta oscillations are involved in sensory–motor integration functions [24,25]. Probably, this phase-resetting mechanism acts at a very low cortical processing level. The subject's task was a contrast discrimination, and evidence suggests that it is limited by V1 activity, whose neurons have a contrast threshold [26,27] (unlike those of the retina or lateral geniculate nucleus).

Phase-resetting mechanisms can be also activated by sensory stimuli [8–10]. We compared the effect of a sound-trigger with that of the motor act. Results from *audio-HL* did not show any significant deviation from mean performance in individual subjects or the group-mean. Consequently, if an acoustic phase-resetting modulation of visual oscillations exists [8,10], then it must be lower in amplitude and reliability than the one induced by voluntary action. Comparing the effect of voluntary motor action between the two experiments, we observed that the overall delay of the motor suppression was reduced when using shorter trial intervals (as in experiment 2). This may be a consequence of the different attentional and hazard rate characteristics of the two experiments. It is also possible that attentional allocation not only changes the overall motor-visual timing but also mediates the phase-reset.

Action and visual attention are strongly linked [28–31] and attention can reset the phase of the ongoing activity in visual areas, or exert an oscillatory gain of the sensory processing [32–35]. However, visual attention was clearly allocated also in the *random-HL* condition in experiment 1. Crucially, it was identical between the *audio-HL* and the *self-trigger* conditions of experiment 2. Nevertheless, we did not observe the suppressive motor effect neither in the *random-HL* nor in the *audio-HL* conditions. If attention has a role in promoting oscillation [33,35], it must be tightly coupled with the motor system to explain the present data. It is likely that attention is the common mechanism synchronizing the motor and the visual system and its gain, if modulated in time, generates the oscillation observed here.

Besides the role of attention and voluntary motor action, other mechanisms could be involved in generating visual oscillations. Microsaccades might enhance or suppress visual sensitivity, depending on the stimulus spatio-temporal characteristics [36,37]. Microsaccade rate increases around the start of a voluntary action [38], but the increase is too early and too weak to explain the suppressive effect shown here. Microsaccades possess an intrinsic rhythmicity at around 2–3 Hz. This is a frequency range much lower than the one reported here, making the contribution of microsaccades unlikely. Although we cannot completely exclude the role of microsaccades, our result would indicate that microsaccadic frequency oscillation should be synchronized with the preparatory activity of a hand voluntary action and not with a sound cue or another visual cue (see also Tomassini *et al.* [2]).

We measured visual oscillations in photopic and mesopic vision and found that both are in the theta range. Surprisingly, the frequency was higher in mesopic than photopic conditions (7 versus 5 Hz). This is in striking contrast with temporal frequency neuronal selectivity that shifts towards lower values at low luminance [39,40] and with neuronal temporal processing that is slower at lower luminance [41]. If visual oscillations are a consequence of the endogenous rhythms of the visual cortex [2] being phase-reset by action preparation, then the most likely frequency of the visual oscillation should be the lowest with the highest power. Brain rhythms exhibit an enhancement of alpha-power activity at low, compared with high, luminance [17,18]. This increase could induce the shift towards higher frequency of the visual oscillation at mesopic conditions. If so, the frequency shift would imply that the frequency of visual oscillations is determined by endogenous visual rhythms. This conclusion is also consistent with the other important finding of this study: the advance in the first minimum of the oscillations with respect to the action onset. At low-luminance, visual processing is slowed down and delayed. If the frequency of visual oscillations is determined by endogenous rhythms, the response delay should produce an advance of the phase of the oscillation (shorter latency of the minimum) as we observed. Interestingly, the time difference between the two minima for the two luminance conditions is about 30 ± 18 ms, a value consistent with the physiological delay of about 15 ms for each log-unit attenuation of luminance [40,42]. In summary, this interpretation suggests the oscillation frequency is determined by the endogenous rhythms and not by stimulus processing. Although this interpretation may appear counterintuitive against the general idea that slower processing and slower temporal integration should produce a lower frequency oscillation, it fits nicely with the increase of the alpha-band power at low luminance.

Brain alpha-oscillatory activity is generally linked to inhibition of cortical areas, and thus strongly coupled with stimulus processing [43–45]. Indeed, it has been proposed that both the phase and amplitude of alpha activity reflect the amount of inhibitory cortical influxes over the cortex, and consequently, these parameters are strongly correlated with temporal integration processes [46–48]. We could hypothesize that the increase of alpha-band (and hence also of theta) power at low-luminance results from the decrease of cortical inhibition necessary to process optimally the slow temporal response evoked at low luminance. The typical impulse response of cortical neurons comprises two lobes, one excitatory and one inhibitory. At low luminance, the second inhibitory lobe becomes very weak, given the reduced cortical inhibition [41].

Action exerts a profound influence over perception. For example, it has been shown that eye movements generate a strong visual suppression [49]. In general, stimuli triggered by self-initiated actions can exhibit the so called *motor-induced suppression*: a suppression of stimulus processing caused by a gain reduction of neural response [22]. This suppressive effect interacts with sensory areas via feed-forward connections and generates sensory suppression in a time window of a few hundreds of milliseconds after movement. Moreover, action controls also the perceptual temporal properties by influencing the temporal integration timing [50–52]. We found that when the subject intentionally started the trial by an action, contrast discrimination was clearly impaired in the first 100 ms after button-press. Crucially, no suppressive effect was found in the *random-HL* condition or in the *audio-HL* condition. Given that we reported a *motor-induced suppression* on a contrast discrimination task that it is thought to be limited by V1 neuronal processing [26,27], this sensory-motor interaction probably takes place at very low-level cortical processing stages as V1. However, this interpretation seems to falter when we consider the phenomenon across the whole 1 s interval after action: the suppressive dip is only the first of many other rhythmical dips. Present findings may suggest that the *motor-induced visual suppression* does not occur only once, soon after the action, but rhythmically several times. It should be interpreted as an expression of a more general phenomenon of phase-reset of visual oscillations by action.

Taken together, our results suggest that action resets the phase of visual oscillations and that the frequency of such oscillations is modulated by luminance level and governed by endogenous brain rhythm. The functional role of this mechanism is still not clear. We may speculate that higher-theta visual oscillations could play a key role in determining our ability of synchronizing visual–motor processing at different luminance viewing conditions. White *et al.* [53] found that while low-luminance stimuli exhibit delayed processing, the visual–motor system is able to compensate this perceptual lag and accurately synchronize the action with moving dim stimuli. Accordingly, we may speculate that the goal of phase-reset by action of visual oscillations is to achieve maximum sensitivity at a specific time during the action. Indeed, the present oscillations exhibit a minimum within the first 100 ms from the motor action, regardless of the frequency and luminance viewing conditions (figure 4a,b). Interestingly, the synchronization takes place well before action execution [2], possibly allowing reach of visuomotor phase-coherence before action onset. We could even speculate further that this mechanism is tuned to favour vision during specific phases of repetitive moments, such as walking or running with rhythms in the 3–7 Hz range.

5. Conclusion

Visual discrimination thresholds fluctuate rhythmically over time in the theta range with systematic differences in photopic and mesopic light conditions. These visual oscillations are phase-reset by a voluntary action and not by an external sensory stimulus, such as a sound. The visual rhythmic activity could play a key role in optimizing sensory–motor integration, and may be instrumental in achieving a dynamic compensation of the sensory delay at low luminance.

7

rspb.royalsocietypublishing.org Proc. R. Soc. B 283: 20160692

References

1. Spaak E, de Lange FP, Jensen O. 2014 Local entrainment of alpha oscillations by visual stimuli causes cyclic modulation of perception. *J. Neurosci.* **34**, 3536–3544. (doi:10.1523/Jneurosci.4385-13.2014)

2. Tomassini A, Spinelli D, Jacono M, Sandini G, Morrone MC. 2015 Rhythmic oscillations of visual contrast sensitivity synchronized with action. *J. Neurosci.* **35**, 7019–7029. (doi:10.1523/Jneurosci.4568-14.2015)

3. VanRullen R, Koch C. 2003 Is perception discrete or continuous? *Trends Cogn. Sci.* **7**, 207–213. (doi:10.1016/S1364-6613(03)00095-0)

4. Busch NA, Dubois J, VanRullen R. 2009 the phase of ongoing EEG oscillations predicts visual perception. *J. Neurosci.* **29**, 7869–7876. (doi:10.1523/Jneurosci.0113-09.2009)

5. de Lange FP, Rahnev DA, Donner TH, Lau H. 2013 Prestimulus oscillatory activity over motor cortex reflects perceptual expectations. *J. Neurosci.* **33**, 1400–1410. (doi:10.1523/Jneurosci.1094-12.2013)

6. Hanslmayr S, Volberg G, Wimber M, Dalal SS, Greenlee MW. 2013 Prestimulus oscillatory phase at 7 Hz gates cortical information flow and visual perception. *Curr. Biol.* **23**, 2273–2278. (doi:10.1016/j.cub.2013.09.020)

7. Linkenkaer-Hansen K, Nikulin VV, Palva S, Ilmoniemi RJ, Palva JM. 2004 Prestimulus oscillations enhance psychophysical performance in humans. *J. Neurosci.* **24**, 10 186–10 190. (doi:10.1523/Jneurosci.2584-04.2004)

8. Fiebelkorn IC, Foxe JJ, Butler JS, Mercier MR, Snyder AC, Molholm S. 2011 Ready, set, reset: stimulus-locked periodicity in behavioral performance demonstrates the consequences of cross-sensory phase reset. *J. Neurosci.* **31**, 9971–9981. (doi:10.1523/Jneurosci.1338-11.2011)

9. Lakatos P, Chen CM, O'Connell MN, Mills A, Schroeder CE. 2007 Neuronal oscillations and

8

rspb.royalsocietypublishing.org   Proc. R. Soc. B 283: 20160692

multisensory interaction in primary auditory cortex. *Neuron* **53**, 279–292. (doi:10.1016/j.neuron.2006. 12.011)

10. Romei V, Gross J, Thut G. 2012 Sounds reset rhythms of visual cortex and corresponding human visual perception. *Curr. Biol.* **22**, 807–813. (doi:10. 1016/j.cub.2012.03.025)

11. Engel AK, Fries P, Singer W. 2001 Dynamic predictions: oscillations and synchrony in top-down processing. *Nat. Rev. Neurosci.* **2**, 704–716. (doi:10. 1038/35094565)

12. Goodale MA, Milner AD. 1992 Separate visual pathways for perception and action. *Trends Neurosci.* **15**, 20–25. (doi:10.1016/0166-2236(92)90344-8)

13. Haegens S, Nacher V, Luna R, Romo R, Jensen O. 2011 Alpha-oscillations in the monkey sensorimotor network influence discrimination performance by rhythmical inhibition of neuronal spiking. *Proc. Natl Acad. Sci. USA* **108**, 19 377–19 382. (doi:10.1073/ pnas.1117190108)

14. Stenner MP, Bauer M, Haggard P, Heinze HJ, Dolan R. 2014 Enhanced alpha-oscillations in visual cortex during anticipation of self-generated visual stimulation. *J. Cogn. Neurosci.* **26**, 2540–2551. (doi:10.1162/jocn_a_00658)

15. Zanos TP, Mineault PJ, Nasiotis KT, Guitton D, Pack CC. 2015 A sensorimotor role for traveling waves in primate visual cortex. *Neuron* **85**, 615–627. (doi:10.1016/j.neuron.2014.12.043)

16. Wood DK, Gu C, Corneil BD, Gribble PL, Goodale MA. 2015 Transient visual responses reset the phase of low-frequency oscillations in the skeletomotor periphery. *Eur. J. Neurosci.* **42**, 1919–1932. (doi:10. 1111/ejn.12976)

17. Min BK, Jung YC, Kim E, Park JY. 2013 Bright illumination reduces parietal EEG alpha activity during a sustained attention task. *Brain Res.* **1538**, 83–92. (doi:10.1016/j.brainres.2013.09.031)

18. Nathan RD, Hanley J. 1975 Spectral analysis of the EEG recorded during stimulation of the human fovea. *Brain Res.* **91**, 65–77. (doi:10.1016/0006-8993(75)90466-7)

19. Pelli DG. 1997 The VideoToolBox software for visual psychophysics: transforming numbers into movies. *Spat. Vis.* **10**, 437–442. (doi:10.1163/ 156856897X00366)

20. Pascucci D, Megna N, Panichi M, Baldassi S. 2011 Acoustic cues to visual detection: a classification image study. *J. Vis.* **11**, 7. (doi:10.1167/11.6.7)

21. Aliu SO, Houde JF, Nagarajan SS. 2009 Motor-induced suppression of the auditory cortex. *J. Cogn. Neurosci.* **21**, 791–802. (doi:10.1162/jocn.2009.21055)

22. Blakemore SJ, Wolpert DM, Frith CD. 1998 Central cancellation of self-produced tickle sensation. *Nat. Neurosci.* **1**, 635–640. (doi:10.1038/2870)

23. Schafer EW, Marcus MM. 1973 Self-stimulation alters human sensory brain responses. *Science* **181**, 175–177. (doi:10.1126/science.181.4095.175)

24. Bland BH, Oddie SD. 2001 Theta band oscillation and synchrony in the hippocampal formation and associated structures: the case for its role in sensorimotor integration. *Behav. Brain Res.* **127**, 119–136. (doi:10.1016/S0166-4328(01)00358-8)

25. Caplan JB, Madsen JR, Schulze-Bonhage A, Aschenbrenner-Scheibe R, Newman EL, Kahana MJ. 2003 Human theta oscillations related to sensorimotor integration and spatial learning. *J. Neurosci.* **23**, 4726–4736.

26. Boynton GM, Demb JB, Glover GH, Heeger DJ. 1999 Neuronal basis of contrast discrimination. *Vision Res.* **39**, 257–269. (doi:10.1016/S0042-6989(98)00113-8)

27. Campbell FW, Maffei L. 1970 Electrophysiological evidence for the existence of orientation and size detectors in the human visual system. *J. Physiol.* **207**, 635–652. (doi:10.1113/jphysiol.1970. sp009085)

28. Anderson KL, Ding M. 2011 Attentional modulation of the somatosensory mu rhythm. *Neuroscience* **180**, 165–180. (doi:10.1016/j.neuroscience. 2011.02.004)

29. Craighero L, Fadiga L, Rizzolatti G, Umilta C. 1999 Action for perception: a motor-visual attentional effect. *J. Exp. Psychol. Hum.* **25**, 1673–1692. (doi:10.1037/0096-1523.25.6.1673)

30. Gutteling TP, Kenemans JL, Neggers SFW. 2011 Grasping preparation enhances orientation change detection. *PLoS ONE* **6**, e17675. (doi:10.1371/ journal.pone.0017675)

31. Rolfs M, Lawrence BM, Carrasco M. 2013 Reach preparation enhances visual performance and appearance. *Phil. Trans. R. Soc. B* **368**, 20130057. (doi:10.1098/rstb.2013.0057)

32. Dugue L, Marque P, VanRullen R. 2015 Theta oscillations modulate attentional search performance periodically. *J. Cogn. Neurosci.* **27**, 945–958. (doi:10.1162/jocn_a_00755)

33. Fiebelkorn IC, Saalmann YB, Kastner S. 2013 Rhythmic sampling within and between objects despite sustained attention at a cued location. *Curr. Biol.* **23**, 2553–2558. (doi:10.1016/j.cub.2013.10.063)

34. Huang Y, Chen L, Luo H. 2015 Behavioral oscillation in priming: competing perceptual predictions conveyed in alternating theta-band rhythms. *J. Neurosci.* **35**, 2830–2837. (doi:10.1523/Jneurosci. 4294-14.2015)

35. Landau AN, Fries P. 2012 Attention samples stimuli rhythmically. *Curr. Biol.* **22**, 1000–1004. (doi:10. 1016/j.cub.2012.03.054)

36. Martinez-Conde S, Otero-Millan J, Macknik SL. 2013 The impact of microsaccades on vision: towards a unified theory of saccadic function. *Nat. Rev. Neurosci.* **14**, 83–96. (doi:10.1038/nrn3405)

37. Rucci M, Iovin R, Poletti M, Santini F. 2007 Miniature eye movements enhance fine spatial detail. *Nature* **447**, 851–854. (doi:10.1038/ nature05866)

38. Yuval-Greenberg S, Merriam EP, Heeger DJ. 2014 Spontaneous microsaccades reflect shifts in covert attention. *J. Neurosci.* **34**, 13 693–13 700. (doi:10. 1523/JNEUROSCI.0582-14.2014)

39. Burr DC, Holt J, Johnstone JR, Ross J. 1982 Selective depression of motion sensitivity during saccades. *J. Physiol.* **333**, 1–15. (doi:10.1113/jphysiol.1982. sp014434)

40. Julesz B, White B. 1969 Short term visual memory and the pulfrich phenomenon. *Nature* **222**, 639–641. (doi:10.1038/222639a0)

41. Swanson WH, Ueno T, Smith VC, Pokorny J. 1987 Temporal modulation sensitivity and pulse-detection thresholds for chromatic and luminance perturbations. *J. Opt. Soc. Am. A* **4**, 1992–2005. (doi:10.1364/JOSAA.5.001525)

42. Williams JM, Lit A. 1983 Luminance-dependent visual latency for the Hess effect, the Pulfrich effect, and simple reaction time. *Vision Res.* **23**, 171–179. (doi:10.1016/0042-6989(83)90140-2)

43. Dugue L, Marque P, VanRullen R. 2011 The phase of ongoing oscillations mediates the causal relation between brain excitation and visual perception. *J. Neurosci.* **31**, 11 889–11 893. (doi:10.1523/ Jneurosci.1161-11.2011)

44. Jensen O, Gips B, Bergmann TO, Bonnefond M. 2014 Temporal coding organized by coupled alpha and gamma oscillations prioritize visual processing. *Trends Neurosci.* **37**, 357–369. (doi:10.1016/j.tins. 2014.04.001)

45. Scheeringa R, Mazaheri A, Bojak I, Norris DG, Kleinschmidt A. 2011 Modulation of visually evoked cortical fMRI responses by phase of ongoing occipital alpha oscillations. *J. Neurosci.* **31**, 3813–3820. (doi:10.1523/Jneurosci.4697-10.2011)

46. Cecere R, Rees G, Romei V. 2015 Individual differences in alpha frequency drive crossmodal illusory perception. *Curr. Biol.* **25**, 231–235. (doi:10.1016/j.cub.2014.11.034)

47. Lunghi C, Berchicci M, Morrone MC, Di Russo F. 2015 Short-term monocular deprivation alters early components of visual evoked potentials. *J. Physiol. Lond.* **593**, 4361–4372. (doi:10.1113/JP270950)

48. Samaha J, Postle BR. 2015 The speed of alpha-band oscillations predicts the temporal resolution of visual perception. *Curr. Biol.* **25**, 2985–2990. (doi:10.1016/j.cub.2015.10.007)

49. Burr DC, Morrone MC, Ross J. 1994 Selective suppression of the magnocellular visual pathway during saccadic eye-movements. *Nature* **371**, 511–513. (doi:10.1038/371511a0)

50. Cicchini GM, Binda P, Burr DC, Morrone MC. 2013 Transient spatiotopic integration across saccadic eye movements mediates visual stability. *J. Neurophysiol.* **109**, 1117–1125. (doi:10.1152/jn. 00478.2012)

51. Morrone MC, Ross J, Burr D. 2005 Saccadic eye movements cause compression of time as well as space. *Nat. Neurosci.* **8**, 950–954. (doi:10.1038/ nn1488)

52. Wenke D, Haggard P. 2009 How voluntary actions modulate time perception. *Exp. Brain Res.* **196**, 311–318. (doi:10.1007/s00221-009-1848-8)

53. White AL, Linares D, Holcombe AO. 2008 Visuomotor timing compensates for changes in perceptual latency. *Curr. Biol.* **18**, R951–R953. (doi:10.1016/j.cub.2008.08.022)